Altered phenotypic responses of asexual Arctic *Daphnia* after 10 years of rapid climate change

Running Title: Response of asexual *Daphnia* to climate change

Authors:

Athina Karapli-Petritsopoulou[1,2]

Jasmin Josephine Heckelmann[1]

Dörthe Becker[3]

N. John Anderson[4]

Dagmar Frisch[1]

Affiliations:

[1] Department of Evolutionary and Integrative Ecology, Leibniz Institute of Freshwater Ecology and Inland Fisheries (IGB), Berlin, Germany

[2] Department of Biology, Chemistry, Pharmacy, Institute of Biology, Freie Universität Berlin, Berlin, Germany

[3] Naturschutzstation Niederrhein (NABU), Kleve, Germany

[4] Department of Geography & Environment, Loughborough University, Loughborough, UK

Abstract

Understanding the fates of organisms and ecosystems under global change requires consideration of the organisms' rapid adaptation potential. In the Arctic, the recent temperature increase strongly impacts freshwater ecosystems which are important sentinels for climate change. However, a mechanistic understanding of the adaptive capacity of their key zooplankton grazers, among them polyploid, obligate parthenogenetic *Daphnia*, is lacking. Theory suggests low adaptation potential of asexual animals, yet examples exist of asexuals persisting through marked environmental changes. Here, we studied asexual *Daphnia pulicaria* from a meromictic lake in South-West Greenland. Its oxycline hosts purple sulfur bacteria (PSB), a potential food source for *Daphnia*. We tested two key phenotypic traits: (1) thermal tolerance as a response to rapid regional warming and (2) hypoxia tolerance tied to grazing of PSB in the hypoxic/anoxic transition zone. We resurrected *Daphnia* from dormant eggs representing a historical subpopulation from 2011, sampled modern subpopulation representatives in 2022 and measured phenotypic variation of thermal (time to immobilization - T_{imm}) and hypoxia tolerance (respiration rate and critical oxygen limit - P_{crit}) in clonal lineages of both subpopulations. Whole genome sequencing of the tested clonal lineages identified three closely related genetic clusters, one with clones from both subpopulations and two unique to each subpopulation. We observed significantly lower T_{imm} and P_{crit} and a trend for higher respiration rates in the modern subpopulation, indicating a lower tolerance to both high temperature and hypoxia in comparison to the historical subpopulation. As these two traits share common physiological mechanisms, the observed phenotypic divergence might be driven by a relaxed selection pressure on hypoxia tolerance linked to variation in PSB abundance. Our results, while contrary to our

expectation of higher thermal tolerance in the modern subpopulation, provide evidence for phenotypic change within a decade in this asexual *Daphnia* population.

Keywords: freshwater, zooplankton, resurrection ecology, environmental change, phenotypic adaptation, respiration rate, whole genome sequencing, thermal tolerance, hypoxia tolerance, critical oxygen limit

Introduction

Environmental change is a powerful driver of selection and evolutionary adaptation (MacColl 2011; Garant 2020). However, if changes occur too rapidly, the microevolutionary capacity of organisms may fail to track it (Bürger and Lynch 1995; Chevin et al. 2010). Under the current unprecedented rate of environmental change (IPCC 2023) it is unclear which organisms will persist, and under which conditions, as ecosystems are being affected globally (Parmesan 2006; Finn et al. 2023). It is therefore crucial to understand whether and how organisms can adapt at pace with the rapidly changing environments (Visser 2008; Hoffmann and Sgrò 2011).

Growing evidence highlights the significant potential of sexually reproducing organisms for rapid adaptation to climate change (Bradshaw and Holzapfel 2006; Catullo et al. 2019). However, the rapid adaptive capacity of asexual natural populations is still poorly understood (Bast et al. 2018; Jaron et al. 2021). Evolutionary adaptation is facilitated by the process of natural selection acting upon genetic variation (Agashe et al. 2023). To generate this variation, sexual organisms benefit from genetic recombination, a major force in the evolution and establishment of sexual reproduction (Crow 1994). Spontaneous mutations additionally contribute to genetic variation, but are expected to produce mainly deleterious effects, which should constrain mutation rate at an evolutionary low optimum (Kimura 1967). Without the ability for recombination, asexual lineages are thus bound to accumulate non-beneficial mutations in the long term (known as Müller's ratchet), resulting in mutational meltdown (Lynch et al. 1993). Conversely, recent studies of vertebrate and invertebrate asexuals did not find evidence for a reduced fitness of long-lived clones compared with sexual congeners despite the accumulation of mutations (Kočí et al. 2020;

Kearney et al. 2022) and uncovered that the asexual genome is much more dynamic than previously thought including high rates of gene conversion, ameiotic recombination and deletions (Xu et al. 2011; Tucker et al. 2013; Jaron et al. 2021).

The microcrustacean *Daphnia*, a freshwater keystone grazer, is an important model for rapid evolution. Species of this genus generally reproduce by cyclical parthenogenesis (CP), but obligate parthenogenesis (OP) exists, and in higher latitudes is often coupled with polyploidy (Weider 1987; Dufresne and Hebert 1997; Decaestecker et al. 2009). Many studies have evidenced the genetic and phenotypic responses of CP *Daphnia* over centuries and even decades to cultural eutrophication (Frisch et al. 2014), dietary cyanobacteria (Hairston et al. 1999), predation pressure (Cousyn et al. 2001; Chaturvedi et al. 2021), parasites (Decaestecker et al. 2007), salinisation (Wersebe and Weider 2023), and warming (Geerts et al. 2015; Yousey et al. 2018). However, studies in OP *Daphnia* that address the question of rapid adaptation are lacking, especially in Arctic regions where climate change has particularly severe effects.

A powerful method to directly observe evolutionary change in a population across different time periods is known as resurrection ecology. It uses revived dormant stages from natural populations archived in lake sediment (Burge et al. 2018; Weider et al. 2018) for experimental study of otherwise inaccessible phenotypic traits of ancestral populations.

South-West Greenland is a suitable region to test potential contemporary microevolutionary responses, as it has been undergoing particularly pronounced environmental change during the last decades. Average June air temperatures in this region, representing the end of spring thaw, have increased by 2.2°C in the last 30 years, while average summer temperatures (July) increased by 1.1°C in the last 20 years (Saros et al., 2019). Associated

with this average increase of air temperature, there is a trend towards an earlier lake ice-out (Šmejkalová et al. 2016). A recent study in the region of Kangerlussuaq, SW Greenland, showed that the timing of ice-out has implications on the duration of spring mixing and oxygenation of the water column (Hazuková et al. 2024). This area also harbours several oligosaline meromictic lakes (Anderson et al. 2001). These oligotrophic, fishless lakes contain Arctic *Daphnia pulicaria*, a member of the *Daphnia pulex* species complex (Colbourne et al 1998). Following the pattern often observed towards higher latitudes (Beaton and Hebert 1988), *Daphnia* populations in this area are polyploid and obligate parthenogens (asexuals) (Dane et al. 2020).

We focused our study on one of these lakes, Braya Sø, where a single asexual clone has dominated the population for at least the past 200 years (Dane et al. 2020), suggesting a genetically nearly uniform population. An important characteristic of this lake is the presence of phototrophic purple sulfur bacteria (PSB) that form a bacterial plate in the upper part of the anoxic zone. The sediment record indicates that the abundance of PSB is dynamic over time with periods of near absence (McGowan et al. 2008), and that their abundance is correlated with the abundance of ephippia, the dormant stages of *Daphnia* (Anderson et al., submitted). Studies have shown that anaerobic bacteria communities can contribute significantly to crustacean zooplankton diets (Overmann et al. 1999; Kankaala et al. 2010). Moreover, *Daphnia* could be relying on PSB as either a direct or an indirect food source (Massana et al. 1994). To exploit PSB, *Daphnia* require tolerance to hypoxia, to allow them to graze in or near the anoxic zone at least for short periods of time. Hypoxia tolerance could also have implications for thermal tolerance as both traits are strongly associated with the efficiency of oxygen metabolism (Pörtner 2002).

In this study, we asked whether phenotypic evolution in an asexual population is fast enough to track rapid environmental change. Given the recent temperature increase in the area, we tested the possible adaptation of modern clones to higher temperatures. We assessed thermal tolerance by measuring time to immobilisation (T_{imm}) of multiple clonal lineages of two *Daphnia* temporal subpopulations (modern and historical) from Braya Sø. To assess the genotypic variation present in the two temporal subpopulations, we performed whole genome sequencing. Members of the current Braya Sø population had lower respiration rates than populations in neighbouring holomictic lakes (Karapli-Petritsopoulou et al. 2024). To further explore hypoxia tolerance in Braya Sø, we measured respiration rates and determined the critical oxygen limit (P_{crit}) in members of both temporal subpopulations. Respiration rate (i.e. oxygen consumption) was expected to be low in this population to allow feeding on PSB in the hypoxic to anoxic zone (Seidl et al. 2005; Karapli-Petritsopoulou et al. 2024). Similarly, a low P_{crit} would signal high hypoxia tolerance.

Methods

Environmental data

To determine whether there has been a change in summer water temperature at Braya Sø (Lake code: SS4; 66°59'24.1"N 51°01'39.8"W) over the study period, we used the known relationship between ice-out date (IoD; as day of the year) and mean July water temperature (determined by *in situ* data loggers; see Anderson and Brodersen 2001: mean July water temperature = -0.1018*[IoD]+3820.4; r^2: 0.641; $P<0.01$). In the Kangerlussuaq area regional surveys have shown that mean May air temperature [May-T] determines ice-out date: IoD = –2.33*[May-T]+165.24; r^2=0.797; $P<0.05$. May air temperature was taken for

144 the years 2005-2016 from the DMI meteorological station at Kangerlussuaq airport. For the
145 period 2000–2004; (n=5) ice-out date was inferred from *in-situ* data loggers (measuring at
146 either 1 or 2 hourly intervals) confirmed by remote automatic cameras (see Anderson and
147 Brodersen 2001). For the period 2017-2023, ice-out was determined using satellite imagery
148 (Sentinel-2 which has a 2-day return frequency at this latitude (66 °N)); it was not possible
149 to determine ice-out for the lake in 2022 due to cloud cover during the relevant time period.
150 Between 2000 and 2020 ice-out date varied by 29 days (minimum day 141; maximum day
151 170) which gives an inferred mean July water temperature range of 11.04 to 13.77 °C.

152 ## Field sampling

153 Sediment from Braya Sø, South-West Greenland was sampled in April 2022 by extracting
154 three sediment cores with a Hon-Kajak sediment corer (diameter 9 cm), from the deepest
155 part of the lake, one meter apart from each other. Sediment cores were sectioned in the
156 field (0.5 cm interval) and kept at 4 ^{o}C until processing. In July 2022, we sampled adult
157 *Daphnia* from the entire water column using a 200 µm plankton net (diameter 25 cm).
158 Temperature and oxygen profiles of the water column were measured on the day of
159 *Daphnia* sampling (YSI 650 MDS multiprobe). In previous years, a purple sulfur bacteria
160 population was present near the oxycline between 9 and 14 m depth (Anderson,
161 unpublished data). After determining the depth of the oxycline, we sampled the water
162 column at multiple locations in 50 cm increments between 9 and 14 m, using a 5 L Van-Dorn
163 bottle (height 41.5 cm, diameter: 13 cm), but were unable to detect the PSB population.

Sediment core dating

Radiometric dating of the core was performed at the St. Croix Watershed Research Station Minnesota, USA , following the method for Lead-210 dating described in Appleby (2001). Results are shown in Supplementary Table S1.

Resurrection of ephippia from the sediment

Daphnia ephippia were removed from the sediment and decapsulated using watchmaker's forceps. Eggs from individual ephippia were separated into 2 ml SSS-Medium (Saebelfeld et al. 2017). Hatching conditions were 10 °C and a photoperiod of 18:6 light:dark. The resurrected clones used in this study were all hatched from eggs retrieved from the 1 - 1.5 cm sediment section, which was dated to be from 2011 (supplementary table S1). Once hatched, juveniles were transferred to 100 ml jars with SSS-Medium at 14 °C and 24h dimmed light.

Clonal cultures

The clones used in this study were each established from one *Daphnia* female cultured in an incubator at 14 °C under 24 h dimmed light for at least six months before the start of measurements, equivalent to ca. 9 generations. They were fed with 1 mg $C*L^{-1}$ of *Tetradesmus obliquus* (Turpin) M.J. Wynne, 2016 three times a week. For the experiments of this study we used 11 clones representing a historical subpopulation resurrected from a sediment section dated to 2011 and 12 clones representing the modern subpopulation (sampled in summer 2022).

Whole genome sequencing

Genomic DNA extraction from all 11 historical and 12 modern clones was performed using the MasterPure^{TM} Complete DNA and RNA Purification kit (Biozym) according to the manufacturer's instructions. Before DNA extraction, *Daphnia* were treated with a mixture of antibiotics (50 mg/L ampicillin and 50 mg/L tetracycline dissolved in SSS-Medium) and fed with Sephadex G-50 beads (5g*L^{-1}) for two days prior to DNA extraction. Paired-end (PE) sequencing libraries were prepared with the Illumina DNA Prep PCR free method (~300 bp insert size). Sequencing was done on an Illumina NovaSeq 6000 S4 Flowcell with 150bp paired-end-reads and an average of 6 Gb per sample. Library preparation and sequencing were performed at the Competence Centre for Genomic Analysis (CCGA) in Kiel, Germany.

Bioinformatic analyses

Following O'Grady et al. (2022), we used FASTQC 0.11.9 (Andrews 2015) for quality control of PE reads and TrimGalore 0.6.6 (Krueger et al. 2023) for adapter trimming with a Phred score cutoff of 20 and discarding paired reads shorter than 35 bp after trimming. Reads were mapped to the *Daphnia pulex* reference genome (NCBI accession GCF_021134715.1) with BWA-MEM 0.7.17 (Li and Durbin 2009) and default parameters. Duplicate and supplementary reads were removed with *markduplicates* (Picard Toolkit 2.26; Broad Institute 2024) and *samtools view* (Samtools 1.10; Danecek et al. 2021). Single nucleotide polymorphisms (SNPs) were called using *freebayes* 1.3.2 (Garrison and Marth 2012) with a ploidy setting of 3, and excluding regions with extremely high coverage (-g 10,000). For this variant call, only alignments with a mapping quality > 40 and alleles with a base quality > 24 were included. The options –min-alternate-fraction and –min-alternate-count were set to 0.05 and 5, respectively. Next, we filtered variants with vcffilter from vsflib 1.0.3 (Garrison et al. 2022) using the parameters QUAL > 1, QUAL/AO > 10, SAF > 0 and SAR > 0, RPR > 1 and

RPL > 1. The above analyses were conducted within the High-Performance Computing infrastructure at ZEDAT, Freie Universität Berlin (Bennett et al. 2020).

The last stage of filtering and further analysis was performed in R (R Core Team 2023). To obtain the final SNP set we selected polymorphic, biallelic SNPs with a minor allele frequency (MAF) of 0.15 and an average read depth per sample of 10 to 1000 reads using the R package *SeqArray* 1.26.2 (Zheng et al. 2017). From this set we calculated pairwise genome-wide identity-by-state (IBS) similarity with the *snpgdsIBS()* function of the SeqArray package modified for triploid genomes (details in Karapli-Petritsopoulou et al. 2024). The package *SNPrelate* (Zheng et al. 2012) was then used to compute the hierarchical cluster analysis. Principal component analysis (PCA) of SNPs was computed with the package *smartsnp* (Herrando-Pérez et al. 2021)

Time to immobilization

Daphnia of the 23 clones described above were used for time to immobilisation (T_{imm}) tests. These were conducted in two batches with two experimental runs each. Each batch contained a mixture of randomly chosen clones of both subpopulations. Each run had three replicates of each clone from the respective batch (six replicates per clone in total). T_{imm} was measured on pre-adults, aged 10-18 days.

Measurement setup

To measure T_{imm} we used a custom-made apparatus following the design from Burton et al. (2018). The apparatus consisted of 45 6 ml vials with 1.6 cm diameter and 4 cm height that were fitted in a plexiglass box of 28.5 cm x 17.5 cm x 5.5 cm in dimensions in five rows of 9 vials. The box was sealed with silicon and connected to a refrigerated water circulator through two main openings as inflow and outflow on two sides. The two openings were

separated into five smaller ones per side placed between the rows of vials to allow for optimal water flow and temperature control.

Determination of CT_{Max}

To establish the temperature of the T_{imm} assay we first determined average CT_{Max} in mixed clone pre-adults from Braya Sø. For this test we used the apparatus described above connected to the refrigerated water circulator. *Daphnia* were placed individually in each vial and were observed throughout the trial. Starting from 18 °C we increased the water temperature by 1 °C every 6 minutes. The CT_{Max} was reached when all *Daphnia* exhibited immobilisation due to thermal stress, and was determined as 36 °C for the Braya Sø *Daphnia*.

T_{imm} measurement

We measured T_{imm} on pre-adult *Daphnia* at 34 °C (two degrees below CT_{Max}), following Burton et al. (2018). *Daphnia* were placed individually into the vials in a randomised order and the temperature was increased from 18 °C to 34 °C within 16 minutes to avoid a sudden heat shock. *Daphnia* swimming activity was recorded using a Sony Alpha AIII camera with a Tamron HA036 objective mounted on a camera tripod (Hitchy, Hitchy Handy Stativ). A light table (HSK, A4 LIGHT PAD) was positioned beneath the plate to enhance visibility. After all *Daphnia* had reached T_{imm}, they were removed from the apparatus and photographed under a dissecting scope (ZEISS, STEMI 508) at a magnification of 25x using the image analysis software MikroLive v.5 (https://www.mikroskopie.de/). Body length was measured from the top of the head to the apical base of the spine. T_{imm} of individual *Daphnia* was determined using the video material and defined as the moment when no movement was detected for at least 30 seconds.

Respiration rate

Respirometry setup

To estimate the respiration rate and the critical oxygen limit (P_{crit}) of single *Daphnia* we measured oxygen consumption at 18 °C for six hours using a closed respirometry system (Loligo® Systems, Denmark) consisting of a 200 µl 24-well plate fitted with oxygen sensor spots and an SDR SensorDish® Reader (PreSens Precision Sensing GmbH, Germany). The plate was sealed with a PCR film. Before adding individual *Daphnia* to each well, they were filled with SSS medium. Air bubbles were removed from the wells which were then topped up with medium before sealing the plate. To achieve a stable temperature, the 24-well plate was immersed in a sealed flow-through waterbath (Loligo® Systems, Denmark) connected to a circulating refrigerated system (circulator: Thermo Scientific™ HAAKE A10, thermostat: Thermo Scientific™ HAAKE SC100). The MicroResp™ software (Loligo® Systems, Denmark) was used to conduct the measurements.

To account for diffusion of oxygen through the PCR film, we measured oxygen differences at 18 °C in a separate run without *Daphnia* over four hours by placing air-saturated medium in the wells and corrected the measurements with the diffusion rate (see below).

Due to the low fecundity and long time to maturation (aprox. 20 days) of *Daphnia* from the study lake, entering all clones in the measurements synchronously was not possible. We therefore performed the measurements within six weeks in two batches: one including all resurrected (historical) clones and one with the clones collected from the water column in 2022 (modern clones). To control for possible batch effects, the historical clone SS4-5 was included in both batches as a reference. We used pre-adults of 11 to 20 days old for our measurements.

To measure *Daphnia* oxygen consumption, we separated each batch into six runs that were performed during six consecutive days. Each run included one replicate of each clone present in the batch, four replicates of the reference and four blank wells containing medium from the *Daphnia* jars to account for microbial (background) respiration, yielding a total of six replicates per clone. The positions of the clones in the plate were randomized before each run using the Microresp software. After six hours, we measured the body length of individual *Daphnia* as decribed above. In cases when a replicate was missing from a run due to handling, an extra replicate of the same clone was included into the next run.

Statistical data analysis

All statistical analyses were performed in R (v. 4.3.0; R Core Team 2023).

T_{imm}

Daphnia identified as males and female *Daphnia* with eggs were excluded from further analysis, as their different physiological state might have biased the results. Due to this, two clones from the historical subpopulation had to be excluded from further analysis because less than three replicates remained. Additionally, the reference clone SS4-5 was randomly subsampled to six replicates to be included in the analysis. We estimated dry weight from body length of each *Daphnia* using the available Length-Weight formula for this lake's population (Dry Weight = 9.015362 * $Length^{2.86448}$ (Karapli-Petritsopoulou et al. 2024). We fitted two sets of linear mixed models with ML (package lmerTest, v. 3.1-3; Kuznetsova et al. 2017, based on lme4 v. 1.1-33; Bates et al. 2015) and compared them within each set using a Likelihood-Ratio test. The models included either genetic cluster or subpopulation as a fixed factor with the addition of weight in two of the models. The experimental run and clone nested either within genetic cluster or subpopulation were used as random factors:

Set 1:

model gen0: T_{imm} ~ 1 + (1|Run) + (1| Genetic Cluster:Clone)

model gen1: T_{imm} ~ Genetic Cluster + (1|Run) + (1| Genetic Cluster:Clone)

model gen2: T_{imm} ~ Genetic Cluster + Weight + (1|Run) + (1| Genetic Cluster:Clone)

Set 2:

model sub0: T_{imm} ~ 1 + (1|Run) + (1|Subpopulation:Clone)

model sub1: T_{imm} ~ Subpopulation + (1|Run) + (1|Subpopulation:Clone)

model sub2: T_{imm} ~ Subpopulation + Weight + (1|Run) + (1|Subpopulation:Clone)

The models with genetic cluster failed to converge due to the random effect of Clone. We therefore removed the random effect to reduce complexity and reran Set 1 (i.e. model gen1: T_{imm} ~ Genetic Cluster + (1|Run)). The models picked by the Likelihood-Ratio test were re-fitted with REML for reporting.

We used the package multcomp (v. 1.4-25; Hothorn et al. 2008) to perform post-hoc tests with the Holm method for genetic cluster. Data visualisation was performed using the ggplot2 (v. 3.5.1; Wickham 2016) and patchwork (v. 1.2.0; Pedersen 2024) packages.

Respiration rate calculation and statistical analysis

Rates of diffusion, background respiration, and *Daphnia* respiration were calculated with the respR package (v. 2.3.1; Harianto et al. 2019). The respiration rates were adjusted for the mean diffusion rate measured over 24 wells in four hours and the background respiration of each run averaged over the blank wells. We estimated dry weight of *Daphnia* based on their body length using the formula described above and adjusted the respiration

rate dividing by dry weight to obtain weight-specific respiration rate. To correct for batch effect, we used the reference clone SS4-5. For this, we calculated a bias weight as follows:

$$\text{Bias} = \frac{|\overline{ref}_{run} - \overline{ref}|}{\overline{ref}}$$

where $\overline{ref}_{run}$ is the mean mass-specific respiration rate of the reference clone of a given run and $\overline{ref}$ is the overall mean of the reference mass-specific respiration rate. The bias was calculated separately for each of the six runs. To obtain standardised mass-specific respiration rates (in the following $Resp_{standard}$), we multiplied the mass-specific respiration rate of each experimental *Daphnia* with the run-specific bias. The reference clone was randomly subsampled to six replicates to be included in the analysis.

To assess whether genetic cluster or subpopulation were significant factors in explaining our data we performed two model comparisons between a null model with only random effects and a full model containing either genetic cluster or subpopulation as a fixed effect. The random factors were experimental run and clone nested within subpopulation or genetic cluster, respectively. The models were fitted using the lmerTest (v. 3.1-3; Kuznetsova et al. 2017) and the comparisons were done with the Likelihood-Ratio test.

Set 1

model gen0: $Resp_{standard}$ ~ 1 + (1|Run) + (1| Genetic Cluster:Clone)

model gen: $Resp_{standard}$ ~ Genetic Cluster + (1|Run) + (1| Genetic Cluster:Clone)

Set 2

model sub0: $Resp_{standard}$ ~ 1 + (1|Run) + (1| Subpopulation:Clone)

model sub: $Resp_{standard}$ ~ Subpopulation + (1|Run) + (1| Subpopulation:Clone)

Data visualisation was performed with ggplot2 (v. 3.5.1; Wickham 2016) and patchwork (v. 1.2.0; Pedersen 2024).

P_{crit} estimation and statistical analysis

P_{crit} was estimated using the broken stick method from the respR package (v. 2.3.1; Harianto et al. 2019). Many individuals did not reach P_{crit} and this resulted in an unbalanced dataset between runs. Therefore, a linear mixed model approach was not possible. The P_{crit} of genetic clusters and subpopulations was compared with one-way ANOVA and Welch's t-test, respectively. Post-hoc tests were done using the Holm method. We tested the relationship between weight adjusted respiration rates and P_{crit} with a linear regression ($\log(P_{crit}) \sim \log(weight\_adj\_rates)$).

Results

Environmental data

The modelled lake ice-out data show a pattern of increased variability after 2010 with both extreme early and late dates present (Figure 1A). Extreme early and late ice-out dates reflect higher and lower modelled July surface lake water temperatures, respectively (Figure 1B). Exemplary August lake profiles from an average year before the increase in variability (2008) and two years after 2010 with an extremely early (2019) and an extremely late (2022) ice-out date show a deeper oxycline in both years after 2010 with 2019 being the deepest of the two (Figure 1D-E). The thermocline was at its deepest in 2019 followed by 2008 and 2022, matching the order from earlier ice-out to later.

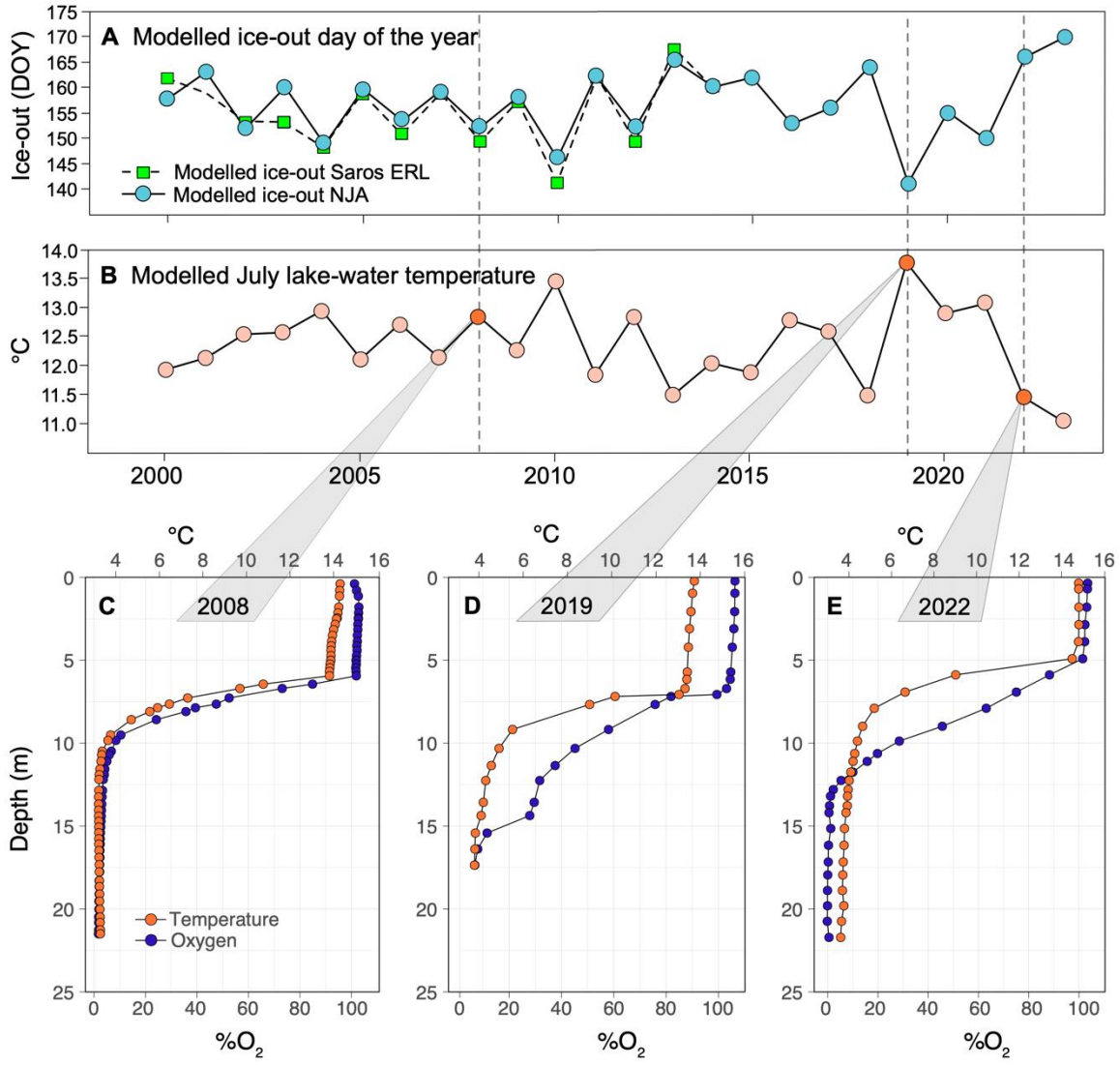

Figure 1. Change in ice-out, temperature and oxygen environment of Braya Sø during the study period. (A) Modelled lake ice-out day of the year (DOY) estimated for this study is shown as blue circles from 2000 to 2023. For comparison, green squares with a dashed line show the ice-out day estimated by Saros et al. (2019). (B) Modelled average July surface lake water temperature. Dashed vertical lines in both (A) and (B) indicate the years 2008, 2019, and 2022, respectively. Depth profiles of August temperature (orange circles) and dissolved oxygen (DO % air saturation, purple circles) in Braya Sø measured in the years 2008 (C), 2019 (D) and 2022 (E).

Genomic results

A total of 365,466 SNPs remained after filtering and were used in further analysis. The hierarchical cluster analysis based on identity-by-state (IBS) identified three closely related genetic clusters: two clusters unique to each temporal subpopulation (a historical cluster with five of the 11 resurrected clones from 2011, and a modern cluster with nine clones

sampled in 2022), and a mixed cluster which included six of the resurrected and three of the 12 modern clones (Fig 2A, Figure S1). The historical and mixed genetic cluster were more similar to each other with a dissimilarity range (1 - IBS) of 8.75% - 11.49%, while their common dissimilarity range to the modern cluster was 8.91% - 13.33% (Table S2). These ranges are relative to the total number of SNPs identified. Based on an estimated genome size of 150 Mb, the highest dissimilarity of ~13% corresponds to a genome-wide IBS of 0.03%. The PCA confirmed the clusters with PCA1 separating mainly the mixed from the modern cluster and explaining 34% of the variation, while PCA2 separated the historical cluster from the other two and explained 14.9% of the variation (Fig. 2B).

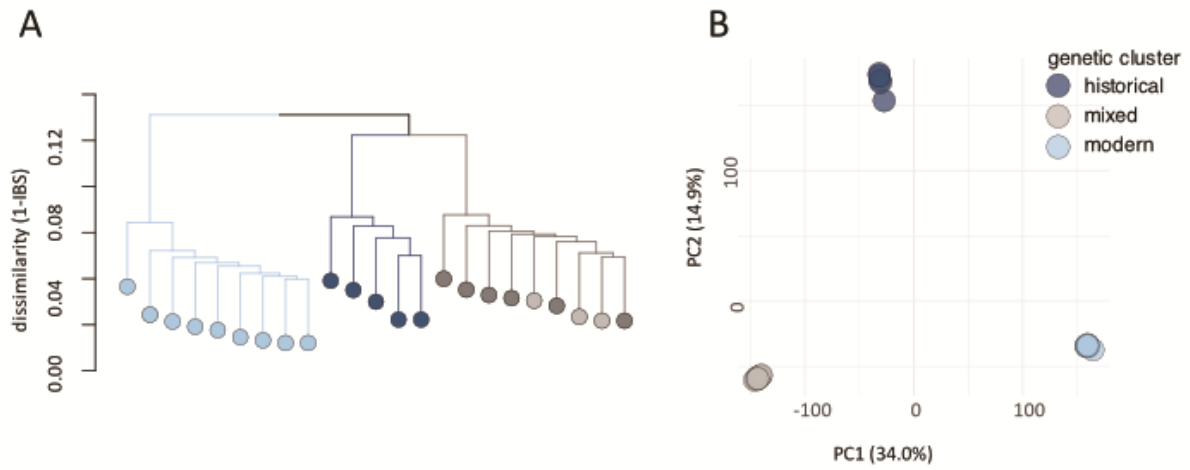

Figure 2. Genetic clusters of clonal lineages based on identity-by-state (IBS). (A) Dendrogram showing the results of hierarchical cluster analysis based on pairwise dissimilarity values (1-IBS). From left to right the modern cluster is represented by light blue circles, the historical cluster by dark blue and the mixed cluster by grey circles. The darker and light grey shade in the mixed cluster represents clonal lineages from the historical and modern subpopulation respectively. Each circle represents one clonal lineage. (B) Principal component analysis (PCA) of all identified SNPs, using the same colour code as the dendrogram with one circle per clone.

Time to immobilization (T_{imm})

Both predictor variables "subpopulation" and "genetic cluster" explained the data variation significantly better than the null model, while the addition of "Weight" as a fixed factor did not improve the model (Table 1a). Time to immobilization (T_{imm}) was significantly lower for the modern genetic cluster compared with the mixed and historical clusters (Fig. 3a, Table 1b, Table S3). Additionally, the modern subpopulation showed a significantly lower T_{imm} compared to the historical subpopulation (Fig. 3b, Table 1c).

Table 1. Model comparison with Likelihood-Ratio Test (**a**) and model results for model gen1 (**b**) and model sub1 (**c**) for time to immobilization (T_{imm}).

a. Model comparisons	**npar**	**AIC**	**BIC**	**logLik**	**deviance**	**Chisq**	**Df**	**Pr(>Chisq)**
Set 1								
null: T_{imm} ~ 1 + (1|Run)	3	1869.76	1877.92	-931.88	1863.76			
gen1: T_{imm} ~ Genetic Cluster + (1|Run)	5	1830.32	1843.91	-910.16	1820.32	43.45	2	**3.675E-10**
gen2: T_{imm} ~ Genetic Cluster + Weight + (1|Run)	6	1832.18	1848.49	-910.09	1820.18	0.13	1	0.715
Set 2								
null: T_{imm} ~ 1 + (1|Run) + (1|Subpopulation:Clone)	4	1855.03	1865.90	-923.51	1847.03			
sub1: T_{imm} ~ Subpopulation + (1|Run) + (1|Subpopulation:Clone)	5	1842.44	1856.03	-916.22	1832.44	14.59	1	**1.333E-04**
sub2: T_{imm} ~ Subpopulation + Weight + (1|Run) + (1|Subpopulation:Clone)	6	1844.36	1860.67	-916.18	1832.36	0.07	1	0.787

b. Model gen1: Timm ~ Genetic Cluster + (1|Run) + (1|Genetic Cluster: Clone)

	Estimate	**Std. Error**	**df**	**t value**	**Pr(>|t|)**
Intercept	2425.86	315.84	9.55	7.68	**2.188E-05**
Genetic cluster mixed	-158.31	250.52	106.71	-0.63	0.529
Genetic cluster modern	-1271.07	255.65	106.97	-4.97	**2.539E-06**

c. Model sub1: Timm ~ Subpopulation + (1|Run) + (1|Subpopulation:Clone)

	Estimate	Std. Error	df	t value	Pr(>|t|)
Intercept	2361.71	253.45	5.39	9.32	**1.594E-04**
Subpopulation modern	-937.63	208.54	18.09	-4.50	**2.765E-04**

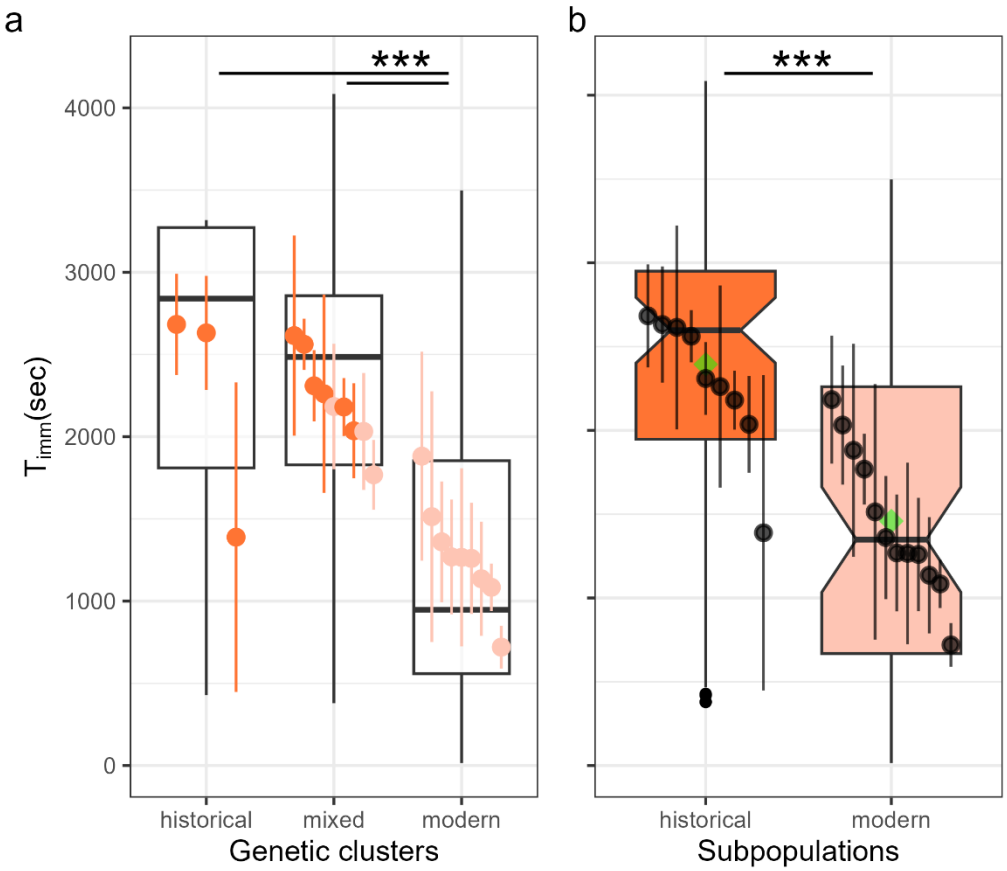

Figure 3. Time to immobilisation (T_{imm}) among genetic clusters (**a**) and between temporal subpopulations (**b**). The darker shades in both panels represent the historical subpopulation and the lighter shades the modern subpopulation. Point ranges in boxplots represent means per clone across replicates with SE. The boxplots are limited by the first and third quartiles, the middle line is the median and the whiskers are 1.5x interquartile ranges. Filled black circles at the bottom end of the whiskers represent outliers. In panel **b** green diamonds indicate mean values per subpopulation. Horizontal bars above the boxes represent post-hoc comparisons between genetic clusters (**a**, Holm method) and subpopulations (**b**, lmm model result). The statistical significance of the p-value is shown by asterisks (*** < 0.001). In panel **a** both comparisons share the same statistical significance.

Respiration rate

We observed a trend for respiration rates to be higher in the modern cluster (historical < mixed < modern) as well as in the modern compared with the historical subpopulation (Fig. 4). These differences, however, were not statistically significant and the null models were selected by the Likelihood-Ratio test in both sets of comparisons (Table 2).

Table 2. Model comparison with Likelihood-Ratio test for respiration data.

Model comparison for genetic cluster	**npar**	**AIC**	**BIC**	**logLik**	**deviance**	**Chisq**	**Df**	**Pr(>Chisq)**
gen0: $Resp_{standard}$ ~ 1 + (1|Run) + (1|Genetic Cluster:Clone)	4	-655.82	-644.17	331.91	-663.82			
gen: $Resp_{standard}$ ~ Genetic Cluster + (1|Run) + (1|Genetic Cluster:Clone)	6	-655.08	-637.60	333.54	-667.08	3.25	2	0.197
Model comparison for subpopulation								
sub0: $Resp_{standard}$ ~ 1 + (1|Run) + (1|Subpopulation:Clone)	4	-655.82	-644.17	331.91	-663.82			
sub: $Resp_{standard}$ ~ Subpopulation + (1|Run) + (1|Subpopulation:Clone)	5	-656.07	-641.50	333.03	-666.07	2.24	1	0.134

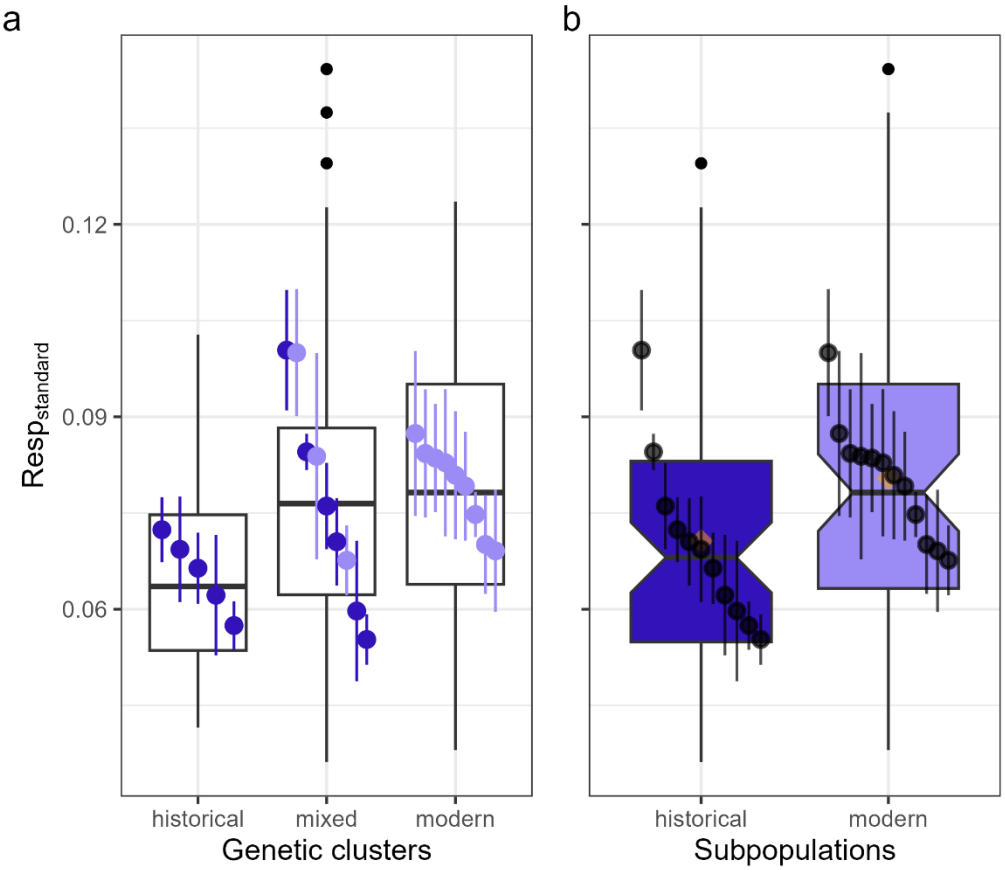

Figure 4. Standardized respiration rate ($Resp_{standard}$) among genetic clusters (**a**) and between temporal subpopulations (**b**). The darker shade in both panels represents the historical subpopulation and the lighter shade the modern subpopulation. Point ranges show the mean of each clone across replicates and the standard error of the mean. The boxplot limits represent the first and third quartiles, the middle line indicating the median, whiskers are 1.5x interquartile ranges. Filled black circles above the whiskers represent outliers. In panel b the mean values of the subpopulations are shown by orange diamonds.

P_{crit}

Most individuals did not reach the critical oxygen limit (P_{crit}) within the 6 h measurement (Fig. 5a, 5c). This was mostly because low oxygen consumption prevented oxygen levels from approaching P_{crit} (see supplementary figure S2). Notably, fewer individuals from the historical subpopulation reached P_{crit}, emphasizing the observed trend for lower respiration rates of the historical subpopulation. The same pattern was observed for the historical genetic cluster. Differences in P_{crit} were significant among genetic clusters ($F_{(2,43)} = 4.72$, p =

0.014) and the modern genetic cluster had a significantly higher P_{crit} than both other clusters (Fig. 5b, Table S4). P_{crit} did not significantly differ between subpopulations (Figure 5d; $t_{(25.52)}$ = -1.1, p = 0.28). Finally, the overall regression between weight-adjusted respiration rates and P_{crit} was statistically significant with a positive relationship between the two (adj. R^2= 0.088, $F_{(1,44)}$ = 5.39, p = 0.024; Figure S3), suggesting a significant association between the two variables.

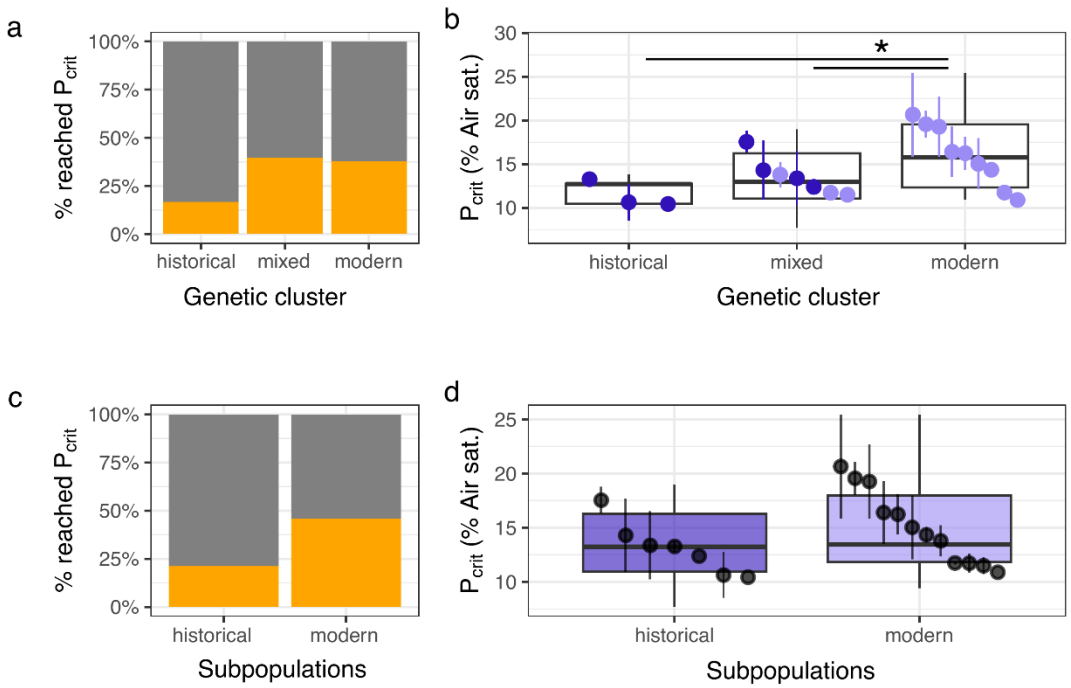

Figure 5. Critical oxygen limit in historical and modern subpopulations. Barplots of the percentage of replicates that reached the critical oxygen limit (P_{crit}) and boxplots of % air saturation values of P_{crit} per genetic cluster (a,b) and subpopulation (c,d). Percentages that reached P_{crit} are shown in orange. The historical and modern subpopulation are represented by darker and lighter purple shades, respectively. Point ranges are the means per clone with SE. The boxplots were computed as in Figure 4. Horizontal bars above the boxes represent post-hoc comparisons between genetic clusters (Holm method). The statistical significance of the p-value is shown by asterisks (* < 0.05). Both comparisons share the same statistical significance.

Discussion

We tested the adaptation potential of an asexual *Daphnia* population in response to rapid environmental change, focussing on temperature rise and its relevance for hypoxia tolerance. For this we applied a resurrection ecology approach to compare two temporal snapshots of this population; resurrected *Daphnia* from a sediment layer dating to 2011 and contemporary clonal lineages from the population sampled in 2022. Whole genome sequencing of all clones participating in the experimental work of this study identified three genetic clusters of which two are specific to each temporal subpopulation, and a third which contains clones of both subpopulations. The genetic clusters and temporal subpopulations provide similar interpretations of the results (except in the case of P_{crit}). We found that modern and historical *Daphnia* differ in both thermal and hypoxia tolerance, albeit at different magnitudes. Contrary to our prediction, T_{imm} was shorter for the modern *Daphnia* (both subpopulation and genetic cluster), a proxy that indicates tolerance to high temperatures. Additionally, we observed slightly higher respiration rates for the modern subpopulation and significantly higher P_{crit} for the modern genetic cluster, both indicating a lower tolerance to hypoxia. The combined pattern of low thermal and hypoxia tolerance points to the shared physiological coping mechanisms that can enhance oxygen uptake (*e.g.*, haemoglobin increase). We discuss these results in the light of the current climate change in the study area that has significant effects on lake stratification and the lakes' oxygen environment (Hazuková et al. 2024).

Our results suggest the occurrence of phenotypic change in an asexual *Daphnia* population within a decade of environmental change among three closely related genetic clusters. The high similarity seen among the clusters (highest pairwise dissimilarity between clusters was

13.33% within the SNP set, equivalent to 0.03% divergence genome-wide) could suggest common ancestry via long-term molecular evolution, however the maximum number of SNPs we found between clusters (13.33% corresponds to 48,717 SNPs) is elevated in comparison to SNPs found between diploid Japanese obligate asexual lineages of *Daphnia pulex* (~5,000), estimated to have diverged molecularly during the last ~300 years based on nuclear substitutions (Ohtsuki et al. 2022). A higher SNP number could partly be explained by the higher mutation rates occurring in polyploids in comparison to diploids (Meirmans et al. 2018). Additionally, even though it is likely that polar regions including Greenland harbour only obligate parthenogenetic *Daphnia* (Weider et al. 1999; Decaestecker et al. 2009; Haileselasie et al. 2016) and sexually reproducing *Daphnia* populations have not (yet) been found in the study area, the possibility of local clonal recruitment through sexual turnover cannot be completely excluded.

Two of the genetic clusters are specific to one of each time periods, and a third has members of both periods. The most likely explanation would be an undetected, local presence of members of the modern cluster at a low frequency in the historical subpopulation, rising in frequency due to clonal selection. Alternatively, dispersal from nearby lakes cannot be excluded. In both cases, the recent change in the clonal frequencies contrast the results of a previous study (Dane et al. 2020) that showed the long-term dominance of a single clone for at least the last 200 years until ~2008, identified by microsatellite markers. A final possibility is that these genetic clusters are all closely related to the dominant clone found previously, with the lower resolution of the microsatellite analysis being unable to detect them.

A lower tolerance to high temperatures as observed in the modern clones (and more pronounced in the modern genetic cluster) while temperature in the area is rising (Saros et al. 2019), contradicts our expectations about the direction of phenotypic change. Climate data point to an increased variability in yearly spring and summer temperatures rather than a linear increase. While several of our August temperature profiles for SS4 do not show an extreme difference in surface water temperatures, earlier ice-out is predicted to lead to a deepening of surface water mixing, resulting in a shift of the thermocline and the oxycline to greater water depths (Hazuková et al. 2024). Our data demonstrate such an expansion of the higher surface temperatures during years of earlier ice-out, thus reducing the thermal refugium for *Daphnia*. Higher temperatures near the water surface do not yet seem to be directly affecting this population as the adaptations to hypoxia present in this population may have shielded it against the recent higher temperature range. Nevertheless, further warming and more frequent early ice-out events in future years, may catch up with the population's thermal tolerance pushing it to a maladapted state.

The lower tolerance to hypoxia observed for the modern subpopulation and especially for the modern genetic cluster may prevent *Daphnia* from successfully grazing near or in the anoxic layer. It has been shown that *Daphnia* can utilize phototrophic purple sulfur bacteria (PSB) as a food source (Jürgens et al. 1994; Massana et al. 1994). *Daphnia's* dependence on PSB which are a supplement to the scarce algal food sources, may be stronger in Braya Sø or other oligotrophic meromictic lakes occurring in the Kangerlussuaq area. However, according to paleolimnological pigment analysis on the lake sediment of Braya Sø, the PSB population has fluctuated in size in the past 500 years and seems to have been declining since 2000 (Dane et al. 2020, Anderson et al., submitted). In line with these data, we were unable to locate the PSB population during field sampling in August 2022, a season when

the bacterial plates of PSB are typically present. The presence of dense PSB bacterial plates in August has for example been observed in Lake Cadagno, an alpine lake with climatic conditions similar to those in West Greenland (Tonolla et al. 2003; Storelli et al. 2024). The deepening of the oxycline observed in the 2019 and 2022 profiles might indicate an important trend occurring since 2010, with early ice-out occurring more frequently. According to Hazuková et al. (2024), earlier ice-out induces more prolonged spring mixing in holomictic lakes before the summer stratification, expanding the presence of oxygen deeper into the water column. Since phototrophic PSB rely on both sufficient light and anoxic conditions (Overmann 2008), this shift in the oxycline is likely to destabilize the PSB population, a situation that could be perpetuated in the following years.

The presence of fish in Braya Sø would be another reason for the *Daphnia* to descend closer to the anoxic zone (Larsson and Lampert 2011). However, bigger *Daphnia* species like the polylpoid Arctic *D. pulicaria* and fish generally do not co-occur in lakes of West Greenland (Jeppesen et al. 2017). Hence, a reduced or absent PSB layer could be a major reason for tolerance to hypoxia no longer conferring an important benefit. The central mechanism for adaptation to hypoxia is through elevated haemoglobin (Hb) production and oxygen affinity (Paul et al. 2004; Seidl et al. 2005). Other mechanisms are changes in carbohydrate-degrading enzymes, and a decrease in oxygen consumption and P_{crit} (Seidl et al. 2005; Zeis et al. 2009). These adaptations involving elevated protein synthesis may confer costs (Pirow et al. 2001), and therefore the relaxation of this selection pressure could explain a lower hypoxia tolerance in the modern subpopulation.

Finally, a similar trend for the two measured traits (low tolerance to hypoxia combined with low thermal tolerance and vice versa) suggests a relationship with the physiological

555 connection of the two traits as explained by the oxygen-limited thermal tolerance
556 hypothesis (Pörtner 2002). This hypothesis posits that the upper thermal limit of an
557 organism is set by oxygen limitation and transportation capacity and has found more
558 support in water-breathing arthropods in comparison to air-breathers (Verberk et al. 2016).
559 This has also been observed in *Daphnia* where elevated oxygen demand caused an increase
560 in Hb production with rising oxygen consumption at higher temperatures, similar to hypoxic
561 conditions (Fox and Phear 1953). Higher gene expression of haemoglobin has been
562 measured as a reaction to both hypoxia and raised temperature (Lamkemeyer et al. 2003;
563 Becker et al. 2011; Zeis 2020), while increased Hb levels were correlated with longer T_{imm}
564 (Yampolsky et al. 2014). This common mechanism suggests that a shift in hypoxia tolerance
565 in response to the environment would also affect thermal tolerance.

566 In conclusion, we observed phenotypic change over a short time period in an asexual
567 population of *Daphnia*. The direction of this change was, however, contrary to our
568 expectation. Even though temperature rise is one of the most prevalent factors of global
569 change, our findings suggest that at least until now temperature was not the driving stress
570 factor for this population. In contrast, the destabilisation of the PSB population and a thus
571 reduced demand for hypoxia tolerance may have outbalanced the costs of hypoxia
572 adaptation such as elevated haemoglobin production, leading simultaneously to a lower
573 thermal tolerance. The consequences of this phenotypic change could increase the
574 population's vulnerability to future warming. This finding further demonstrates the
575 complexity of the impacts of environmental change in ecosystems and how local
576 adaptations to unique environmental factors affect population responses. In addition, we
577 found three genetic clusters in this asexual population that may have resulted from

molecular evolution. Whether these genetic clusters are only found in this lake or have dispersed from other regional lakes is unknown.

Our findings pose the question if the relatively small genome-wide differences among the genomic clusters could explain the associated phenotypic divergence. In future research, it will be important to disentangle the molecular underpinnings, in particular on gene expression profiles, epigenetic modifications or ploidy-related effects which could underlie the observed phenotypes. The presence of such mechanisms could be crucial for asexually reproducing animals to keep up with the contemporary fast-paced environmental change, ultimately allowing their survival.

Author contributions

AKP: Conceptualization (supporting); Formal analysis (lead); Investigation (lead); Methodology (equal); Visualisation (equal); Writing-original draft preparation (lead); Writing-Review & Editing (equal). **JJH**: Investigation (supporting); Methodology (supporting); Writing-Review & Editing (supporting). **DB:** Conceptualization (supporting); Writing-Review & Editing (equal). **NJA:** Conceptualization (supporting); Formal analysis (equal); Resources (supporting); Visualisation (supporting); Writing-Review & Editing (equal). **DF:** Conceptualization (lead); Formal analysis (equal); Funding acquisition (lead); Investigation (supporting); Methodology (supporting); Project administration (lead); Resources (lead); Supervision (lead); Visualisation (equal); Writing-original draft preparation (supporting); Writing-Review & Editing (equal).

Acknowledgements

NGS analyses were carried out at the Competence Centre for Genomic Analysis (Kiel). We thank James Shilland for his immense assistance in the field. We are grateful to the Government of Greenland for granting Prior Informed Consent for utilization of Greenland genetic resources (non-exclusive licence no. G22-076) that permits collection and basic research on genetic resources.

Funding

This research was funded by the Deutsche Forschungsgemeinschaft (DFG, German Research Foundation) – Project number 461099895. Computing resources for bioinformatic analysis were partially funded by the German Federal Ministry of Education and Research (BMBF, Förderkennzeichen 033W034A). DNA sequencing was supported by the DFG Research Infrastructure NGS_CC (project 407495230) as part of the Next Generation Sequencing Competence Network (project 423957469).

References

Agashe, D., M. Sane, and S. Singhal. 2023. Revisiting the Role of Genetic Variation in Adaptation. Am. Nat. **202**: 486–502. doi:10.1086/726012

Anderson, N. J., and K. P. Brodersen. 2001. Determining the date of ice-melt for low Arctic lakes along Søndre Strømfjord, southern West Greenland. Geol. Greenl. Surv. Bull. **189**: 54–59. doi:10.34194/ggub.v189.5156

Anderson, N. J., R. Harriman, D. B. Ryves, and S. T. Patrick. 2001. Dominant Factors Controlling Variability in the Ionic Composition of West Greenland Lakes. Arct. Antarct. Alp. Res. **33**: 418–425. doi:10.1080/15230430.2001.12003450

621 Andrews, S. 2015. FASTQC A Quality Control tool for High Throughput Sequence Data. Babraham
622 Inst.
623 Appleby, P. G. 2001. Chronostratigraphic Techniques in Recent Sediments, p. 171–203. *In* W.M. Last
624 and J.P. Smol [eds.], Tracking Environmental Change Using Lake Sediments: Basin Analysis,
625 Coring, and Chronological Techniques. Springer Netherlands.
626 Bast, J. and others. 2018. Consequences of Asexuality in Natural Populations: Insights from Stick
627 Insects. Mol. Biol. Evol. **35**: 1668–1677. doi:10.1093/molbev/msy058
628 Bates, D., M. Mächler, B. Bolker, and S. Walker. 2015. Fitting Linear Mixed-Effects Models Using
629 lme4. J. Stat. Softw. **67**: 1–48. doi:10.18637/jss.v067.i01
630 Beaton, M. J., and P. D. N. Hebert. 1988. Geographical Parthenogenesis and Polyploidy in Daphnia
631 pulex. Am. Nat. **132**: 837–845. doi:10.1086/284892
632 Becker, D., B. F. Brinkmann, B. Zeis, and R. J. Paul. 2011. Acute changes in temperature or oxygen
633 availability induce ROS fluctuations in Daphnia magna linked with fluctuations of reduced
634 and oxidized glutathione, catalase activity and gene (haemoglobin) expression. Biol. Cell **103**:
635 351–363. doi:10.1042/BC20100145
636 Bennett, L., B. Melchers, and B. Proppe. 2020. Curta: A General-purpose High-Performance
637 Computer at ZEDAT, Freie Universität Berlin.doi:10.17169/refubium-26754
638 Bradshaw, W. E., and C. M. Holzapfel. 2006. Evolutionary Response to Rapid Climate Change. Science
639 **312**: 1477–1478. doi:10.1126/science.1127000
640 Broad Institute. 2024. Picard toolkit.
641 Burge, D. R. L., M. B. Edlund, and D. Frisch. 2018. Paleolimnology and resurrection ecology: The
642 future of reconstructing the past. Evol. Appl. **11**: 42–59. doi:10.1111/eva.12556
643 Bürger, R., and M. Lynch. 1995. Evolution and Extinction in a Changing Environment: A Quantitative-
644 Genetic Analysis. Evolution **49**: 151–163. doi:10.1111/j.1558-5646.1995.tb05967.x
645 Burton, T., B. Zeis, and S. Einum. 2018. Automated measurement of upper thermal limits in small
646 aquatic animals. 1-5. doi:10.1242/jeb.182386

647 Calvin, K. and others. 2023. IPCC, 2023: Climate Change 2023: Synthesis Report. Contribution of
648 Working Groups I, II and III to the Sixth Assessment Report of the Intergovernmental Panel
649 on Climate Change [Core Writing Team, H. Lee and J. Romero (eds.)]. IPCC, Geneva,
650 Switzerland. First. Intergovernmental Panel on Climate Change (IPCC).
651 Catullo, R. A., J. Llewelyn, B. L. Phillips, and C. C. Moritz. 2019. The Potential for Rapid Evolution
652 under Anthropogenic Climate Change. Curr. Biol. **29**: R996–R1007.
653 doi:10.1016/j.cub.2019.08.028
654 Chaturvedi, A. and others. 2021. Extensive standing genetic variation from a small number of
655 founders enables rapid adaptation in Daphnia. Nat. Commun. **12**: 4306. doi:10.1038/s41467-
656 021-24581-z
657 Chevin, L.-M., R. Lande, and G. M. Mace. 2010. Adaptation, Plasticity, and Extinction in a Changing
658 Environment: Towards a Predictive Theory. PLOS Biol. **8**: e1000357.
659 doi:10.1371/journal.pbio.1000357
660 Cousyn, C., L. De Meester, J. K. Colbourne, L. Brendonck, D. Verschuren, and F. Volckaert. 2001.
661 Rapid, local adaptation of zooplankton behavior to changes in predation pressure in the
662 absence of neutral genetic changes. Proc. Natl. Acad. Sci. **98**: 6256–6260.
663 doi:10.1073/PNAS.111606798
664 Crow, J. F. 1994. Advantages of sexual reproduction. Dev. Genet. **15**: 205–213.
665 doi:10.1002/dvg.1020150303
666 Dane, M., N. J. Anderson, C. L. Osburn, J. K. Colbourne, and D. Frisch. 2020. Centennial clonal
667 stability of asexual Daphnia in Greenland lakes despite climate variability. Ecol. Evol. **10**:
668 14178–14188. doi:10.1002/ece3.7012
669 Danecek, P. and others. 2021. Twelve years of SAMtools and BCFtools. GigaScience **10**: giab008.
670 doi:10.1093/gigascience/giab008
671 Decaestecker, E., L. De Meester, and J. Mergeay. 2009. Cyclical Parthenogenesis in Daphnia: Sexual
672 Versus Asexual Reproduction, p. 295–316. *In* Lost Sex. Springer Netherlands.

673 Decaestecker, E., S. Gaba, J. A. M. Raeymaekers, R. Stoks, L. Van Kerckhoven, D. Ebert, and L. De
674 Meester. 2007. Host–parasite 'Red Queen' dynamics archived in pond sediment. Nat. 2007
675 4507171 **450**: 870–873. doi:10.1038/nature06291
676 Dufresne, F., and P. D. N. Hebert. 1997. Pleistocene glaciations and polyphyletic origins of polyploidy
677 in an arctic cladoceran. Proc. R. Soc. Lond. B Biol. Sci. **264**: 201–206.
678 doi:10.1098/rspb.1997.0028
679 Finn, C., F. Grattarola, and D. Pincheira-Donoso. 2023. More losers than winners: investigating
680 Anthropocene defaunation through the diversity of population trends. Biol. Rev. **98**: 1732–
681 1748. doi:10.1111/brv.12974
682 Fox, H. M., and E. A. Phear. 1953. Factors influencing haemoglobin synthesis by Daphnia. Proc. R.
683 Soc. Lond. Ser. B - Biol. Sci. **141**: 179–189. doi:10.1098/rspb.1953.0034
684 Frisch, D., P. K. Morton, P. R. Chowdhury, B. W. Culver, J. K. Colbourne, L. J. Weider, and P. D.
685 Jeyasingh. 2014. A millennial-scale chronicle of evolutionary responses to cultural
686 eutrophication in Daphnia. Ecol. Lett. **17**: 360–368. doi:10.1111/ele.12237
687 Garant, D. 2020. Natural and human-induced environmental changes and their effects on adaptive
688 potential of wild animal populations. Evol. Appl. **13**: 1117. doi:10.1111/eva.12928
689 Garrison, E., Z. N. Kronenberg, E. T. Dawson, B. S. Pedersen, and P. Prins. 2022. A spectrum of free
690 software tools for processing the VCF variant call format: vcflib, bio-vcf, cyvcf2, hts-nim and
691 slivar. PLOS Comput. Biol. **18**: 1–15. doi:10.1371/journal.pcbi.1009123
692 Garrison, E., and G. Marth. 2012. Haplotype-based variant detection from short-read
693 sequencing.doi:10.48550/arXiv.1207.3907
694 Geerts, A. N. and others. 2015. Rapid evolution of thermal tolerance in the water flea Daphnia. Nat.
695 Clim. Change **5**: 665–668. doi:10.1038/nclimate2628
696 Haileselasie, T. H. and others. 2016. Environment not dispersal limitation drives clonal composition
697 of Arctic Daphnia in a recently deglaciated area. Mol. Ecol. **25**: 5830–5842.
698 doi:10.1111/mec.13843

699 Hairston, N. G. and others. 1999. Rapid evolution revealed by dormant eggs. Nature **401**: 446–446.
700 doi:10.1038/46731
701 Harianto, J., N. Carey, and M. Byrne. 2019. respR — An R package for the manipulation and analysis
702 of respirometry data. Methods Ecol. Evol. **10**: 912–920. doi:10.1111/2041-210X.13162
703 Hazuková, V., B. T. Burpee, R. M. Northington, N. J. Anderson, and J. E. Saros. 2024. Earlier ice melt
704 increases hypolimnetic oxygen despite regional warming in small Arctic lakes. Limnol.
705 Oceanogr. Lett. **9**: 258–267. doi:10.1002/lol2.10386
706 Herrando-Pérez, S., R. Tobler, and C. D. Huber. 2021. smartsnp, an r package for fast multivariate
707 analyses of big genomic data. Methods Ecol. Evol. **12**: 2084–2093. doi:10.1111/2041-
708 210X.13684
709 Hoffmann, A. A., and C. M. Sgrò. 2011. Climate change and evolutionary adaptation. Nature **470**:
710 479–485. doi:10.1038/nature09670
711 Hothorn, T., F. Bretz, and P. Westfall. 2008. Simultaneous Inference in General Parametric Models.
712 Biom. J. **50**: 346–363. doi:10.1002/bimj.200810425
713 Jaron, K. S., J. Bast, R. W. Nowell, T. R. Ranallo-Benavidez, M. Robinson-Rechavi, and T. Schwander.
714 2021. Genomic Features of Parthenogenetic Animals. J. Hered. **112**: 19–33.
715 doi:10.1093/jhered/esaa031
716 Jeppesen, E. and others. 2017. The structuring role of fish in Greenland lakes: an overview based on
717 contemporary and paleoecological studies of 87 lakes from the low and the high Arctic.
718 Hydrobiologia **800**: 99–113. doi:10.1007/s10750-017-3279-z
719 Jürgens, K., J. M. Gasol, R. Massana, and C. Pedròs-Aliò. 1994. Control of heterotrophic bacteria and
720 protozoans by Daphnia pulex in the epilimnion of Lake Cisó. Arch. Für Hydrobiol. **131**: 55–78.
721 Kankaala, P., S. Taipale, L. Li, and R. I. Jones. 2010. Diets of crustacean zooplankton, inferred from
722 stable carbon and nitrogen isotope analyses, in lakes with varying allochthonous dissolved
723 organic carbon content. Aquat. Ecol. **44**: 781–795. doi:10.1007/s10452-010-9316-x

Karapli-Petritsopoulou, A., J. J. Heckelmann, N. J. Anderson, S. Franzenburg, and D. Frisch. 2024. Phenotypic divergence associated with genomic changes suggest local adaptation in obligate asexuals. 2024.08.15.608098. doi:10.1101/2024.08.15.608098

Kearney, M. R., M. E. Jasper, V. L. White, I. J. Aitkenhead, M. J. Blacket, J. D. Kong, S. L. Chown, and A. A. Hoffmann. 2022. Parthenogenesis without costs in a grasshopper with hybrid origins. Science **376**: 1110–1114. doi:10.1126/science.abm1072

Kimura, M. 1967. On the evolutionary adjustment of spontaneous mutation rates. Genet. Res. **9**: 23–34. doi:10.1017/S0016672300010284

Kočí, J. and others. 2020. No evidence for accumulation of deleterious mutations and fitness degradation in clonal fish hybrids: Abandoning sex without regrets. Mol. Ecol. **29**: 3038–3055. doi:10.1111/mec.15539

Krueger, F., F. James, P. Ewels, E. Afyounian, M. Weinstein, B. Schuster-Boeckler, G. Hulselmans, and sclamons. 2023. FelixKrueger/TrimGalore: v0.6.10 - add default decompression path.doi:10.5281/zenodo.7598955

Kuznetsova, A., P. B. Brockhoff, and R. H. B. Christensen. 2017. lmerTest package: Tests in linear mixed effects models. J. Stat. Softw. **82**: 1–26. doi:10.18637/jss.v082.i13

Lamkemeyer, T., B. Zeis, and R. J. Paul. 2003. Temperature acclimation influences temperature-related behaviour as well as oxygen-transport physiology and biochemistry in the water flea Daphnia magna. Can. J. Zool. **81**: 237–249. doi:10.1139/z03-001

Larsson, P., and W. Lampert. 2011. Experimental evidence of a low-oxygen refuge for large zooplankton. Limnol. Oceanogr. **56**: 1682–1688. doi:10.4319/lo.2011.56.5.1682

Li, H., and R. Durbin. 2009. Fast and accurate short read alignment with Burrows-Wheeler transform. Bioinforma. Oxf. Engl. **25**: 1754–1760. doi:10.1093/bioinformatics/btp324

Lynch, M., R. Bürger, D. Butcher, and W. Gabriel. 1993. The Mutational Meltdown in Asexual Populations. J. Hered. **84**: 339–344. doi:10.1093/oxfordjournals.jhered.a111354

MacColl, A. D. C. 2011. The ecological causes of evolution. Trends Ecol. Evol. **26**: 514–522. doi:10.1016/j.tree.2011.06.009

Massana, R., J. M. Gasol, K. Jürgens, and C. Pedròs-Aliò. 1994. Impact of Daphnia pulex on a metalimnetic microbial community. J. Plankton Res. **16**: 1379–1399. doi:10.1093/plankt/16.10.1379

McGowan, S., R. K. Juhler, and N. J. Anderson. 2008. Autotrophic response to lake age, conductivity and temperature in two West Greenland lakes. J. Paleolimnol. **39**: 301–317. doi:10.1007/s10933-007-9105-2

Meirmans, P. G., S. Liu, and P. H. van Tienderen. 2018. The Analysis of Polyploid Genetic Data. J. Hered. **109**: 283–296. doi:10.1093/jhered/esy006

Ohtsuki, H., H. Norimatsu, T. Makino, and J. Urabe. 2022. Invasions of an obligate asexual daphnid species support the nearly neutral theory. Sci. Rep. **12**: 7305. doi:10.1038/s41598-022-11218-4

Overmann, J. 2008. Ecology of Phototrophic Sulfur Bacteria, p. 375–396. *In* R. Hell, C. Dahl, D. Knaff, and T. Leustek [eds.], Sulfur Metabolism in Phototrophic Organisms. Advances in Photosynthesis and Respiration, vol 27.

Overmann, J., K. J. Hall, T. G. Northcote, and J. T. Beatty. 1999. Grazing of the copepod Diaptomus connexus on purple sulphur bacteria in a meromictic salt lake. Environ. Microbiol. **1**: 213–221. doi:10.1046/j.1462-2920.1999.00026.x

Parmesan, C. 2006. Ecological and Evolutionary Responses to Recent Climate Change. Annu. Rev. Ecol. Evol. Syst. **37**: 637–669. doi:10.1146/annurev.ecolsys.37.091305.110100

Paul, R. J., B. Zeis, T. Lamkemeyer, M. Seidl, and R. Pirow. 2004. Control of oxygen transport in the microcrustacean Daphnia: regulation of haemoglobin expression as central mechanism of adaptation to different oxygen and temperature conditions. Acta Physiol. Scand. **182**: 259–275. doi:10.1111/j.1365-201X.2004.01362.x

Pedersen, T. L. 2024. patchwork: The composer of plots. manual.

775 Pirow, R., C. Bäumer, and R. J. Paul. 2001. Benefits of haemoglobin in the cladoceran crustacean
776 Daphnia magna. J. Exp. Biol. **204**: 3425–3441. doi:10.1242/jeb.204.20.3425
777 Pörtner, H. O. 2002. Climate variations and the physiological basis of temperature dependent
778 biogeography: systemic to molecular hierarchy of thermal tolerance in animals. Comp.
779 Biochem. Physiol. A. Mol. Integr. Physiol. **132**: 739–761. doi:10.1016/S1095-6433(02)00045-
780 4
781 R Core Team. 2023. R: a language and environment for statistical computing. manual R Foundation
782 for Statistical Computing.
783 Saebelfeld, M., L. Minguez, J. Griebel, M. O. Gessner, and J. Wolinska. 2017. Humic dissolved organic
784 carbon drives oxidative stress and severe fitness impairments in Daphnia. Aquat. Toxicol.
785 **182**: 31–38. doi:10.1016/j.aquatox.2016.11.006
786 Saros, J. E. and others. 2019. Arctic climate shifts drive rapid ecosystem responses across the West
787 Greenland landscape. Environ. Res. Lett. **14**: 074027. doi:10.1088/1748-9326/ab2928
788 Seidl, M. D., R. J. Paul, and R. Pirow. 2005. Effects of hypoxia acclimation on morpho-physiological
789 traits over three generations of Daphnia magna. J. Exp. Biol. **208**: 2165–2175.
790 doi:10.1242/jeb.01614
791 Šmejkalová, T., M. E. Edwards, and J. Dash. 2016. Arctic lakes show strong decadal trend in earlier
792 spring ice-out. Sci. Rep. **6**: 38449. doi:10.1038/srep38449
793 Storelli, N., O. S. Steiner, F. D. Nezio, S. Roman, A. Buetti-Dinh, and D. Bouffard. 2024. Ecological
794 dynamics of anoxygenic microorganisms in stably redox-stratified waters: Intra and inter-
795 seasonal variability of Lake Cadagno.doi:10.21203/rs.3.rs-3358324/v1
796 Tonolla, M., S. Peduzzi, D. Hahn, and R. Peduzzi. 2003. Spatio-temporal distribution of phototrophic
797 sulfur bacteria in the chemocline of meromictic Lake Cadagno (Switzerland). FEMS
798 Microbiol. Ecol. **43**: 89–98. doi:10.1111/j.1574-6941.2003.tb01048.x

Tucker, A. E., M. S. Ackerman, B. D. Eads, S. Xu, and M. Lynch. 2013. Population-genomic insights into the evolutionary origin and fate of obligately asexual Daphnia pulex. Proc. Natl. Acad. Sci. **110**: 15740–15745. doi:10.1073/pnas.1313388110

Verberk, W. C. E. P., J. Overgaard, R. Ern, M. Bayley, T. Wang, L. Boardman, and J. S. Terblanche. 2016. Does oxygen limit thermal tolerance in arthropods? A critical review of current evidence. Comp. Biochem. Physiol. A. Mol. Integr. Physiol. **192**: 64–78. doi:10.1016/j.cbpa.2015.10.020

Visser, M. E. 2008. Keeping up with a warming world; assessing the rate of adaptation to climate change. Proc. R. Soc. B Biol. Sci. **275**: 649–659. doi:10.1098/rspb.2007.0997

Weider, L. J. 1987. Life history variation among low-arctic clones of obligately parthenogenetic Daphnia pulex: a diploid-polyploid complex. Oecologia **73**: 251–256. doi:10.1007/BF00377515

Weider, L. J., A. Hobæk, J. K. Colbourne, T. J. Crease, F. Dufresne, and P. D. N. Hebert. 1999. Holarctic Phylogeography of an asexual species complex I. Mitochondrial DNA variation in arctic Daphnia. Evolution **53**: 777–792. doi:10.1111/j.1558-5646.1999.tb05372.x

Weider, L. J., P. D. Jeyasingh, and D. Frisch. 2018. Evolutionary aspects of resurrection ecology: Progress, scope, and applications—An overview. Evol. Appl. **11**: 3–10. doi:10.1111/eva.12563

Wersebe, M. J., and L. J. Weider. 2023. Resurrection genomics provides molecular and phenotypic evidence of rapid adaptation to salinization in a keystone aquatic species. Proc. Natl. Acad. Sci. **120**: e2217276120. doi:10.1073/pnas.2217276120

Wickham, H. 2016. ggplot2: Elegant graphics for data analysis, Springer-Verlag New York.

Xu, S., A. R. Omilian, and M. E. Cristescu. 2011. High Rate of Large-Scale Hemizygous Deletions in Asexually Propagating Daphnia: Implications for the Evolution of Sex. Mol. Biol. Evol. **28**: 335–342. doi:10.1093/molbev/msq199

824 Yampolsky, L. Y., T. M. M. Schaer, and D. Ebert. 2014. Adaptive phenotypic plasticity and local
825 adaptation for temperature tolerance in freshwater zooplankton. Proc. R. Soc. B Biol. Sci.
826 **281**: 20132744. doi:10.1098/rspb.2013.2744
827 Yousey, A. M., P. R. Chowdhury, N. Biddinger, J. H. Shaw, P. D. Jeyasingh, and L. J. Weider. 2018.
828 Resurrected 'ancient' Daphnia genotypes show reduced thermal stress tolerance compared
829 to modern descendants. R. Soc. Open Sci. **5**: 172193. doi:10.1098/rsos.172193
830 Zeis, B. and others. 2009. Acclimatory responses of the Daphnia pulex proteome to environmental
831 changes. I. Chronic exposure to hypoxia affects the oxygen transport system and
832 carbohydrate metabolism. BMC Physiol. **9**. doi:10.1186/1472-6793-9-7
833 Zeis, B. 2020. Hemoglobin in Arthropods—Daphnia as a Model, p. 163–194. *In* U. Hoeger and J.R.
834 Harris [eds.], Vertebrate and Invertebrate Respiratory Proteins, Lipoproteins and other Body
835 Fluid Proteins. Springer International Publishing.
836 Zheng, X., S. M. Gogarten, M. Lawrence, A. Stilp, M. P. Conomos, B. S. Weir, C. Laurie, and D. Levine.
837 2017. SeqArray—a storage-efficient high-performance data format for WGS variant calls.
838 Bioinformatics **33**: 2251–2257. doi:10.1093/bioinformatics/btx145
839 Zheng, X., D. Levine, J. Shen, S. M. Gogarten, C. Laurie, and B. S. Weir. 2012. A high-performance
840 computing toolset for relatedness and principal component analysis of SNP data.
841 Bioinformatics **28**: 3326–3328. doi:10.1093/bioinformatics/bts606
842

Supplementary Material

Altered phenotypic responses of asexual Arctic *Daphnia* after 10 years of rapid climate change

Authors:

Athina Karapli-Petritsopoulou[1,2], Jasmin Josephine Heckelmann[1], Dörthe Becker[3], N. John Anderson[4],

Dagmar Frisch[1]

Affiliations:

[1] Department of Evolutionary and Integrative Ecology, Leibniz Institute of Freshwater Ecology and Inland Fisheries (IGB), Berlin, Germany

[2] Department of Biology, Chemistry, Pharmacy, Institute of Biology, Freie Universität Berlin, Berlin, Germany

[3] Naturschutzstation Niederrhein (NABU), Kleve, Germany

[4] Department of Geography & Environment, Loughborough University, Loughborough, UK

Supplementary Figures

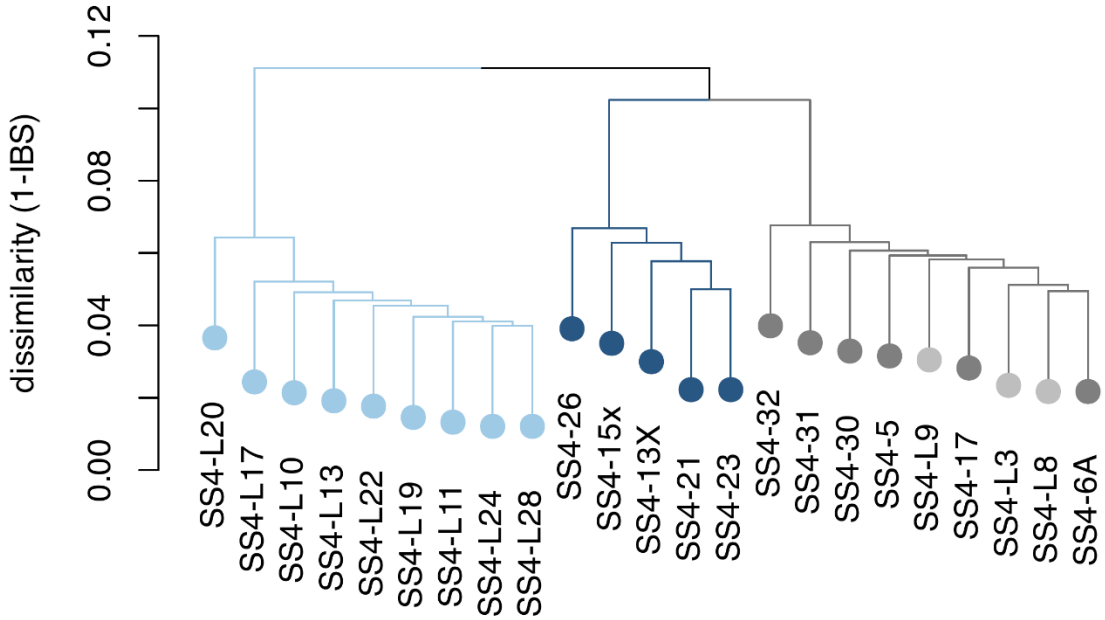

Figure S1. Dendrogram of genetic clusters of clonal lineages based on identity-by-state (IBS) labeled for clone. Dark and light shades represent historical and modern clones respectively. The historical cluster is shown in dark blue, the modern cluster in light blue and the mixed cluster in grey.

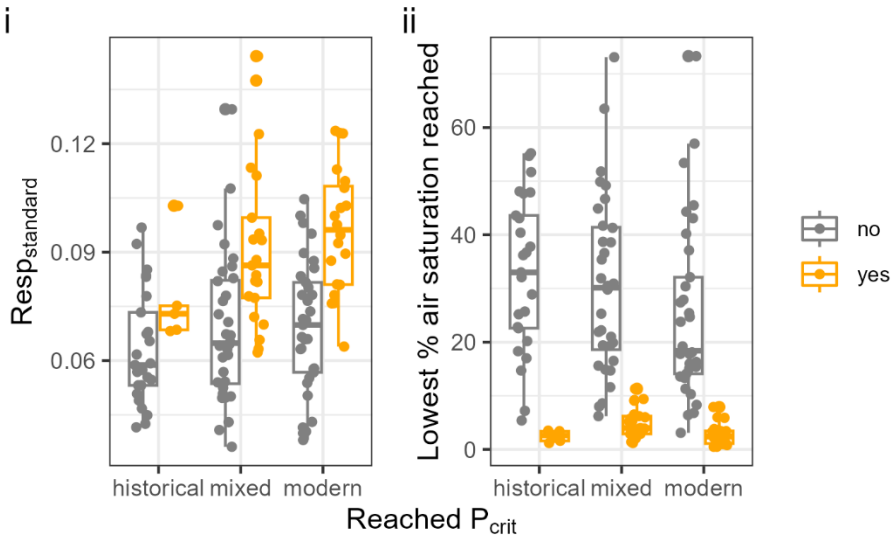

Figure S2. Resp$_{standard}$ (i) and lowest % air saturation value reached at the end of six hours (ii) per genetic cluster according to whether individuals reached P$_{crit}$. Individuals where P$_{crit}$ was successfully measured are coloured with orange, while grey points show non-obtained P$_{crit}$ data.

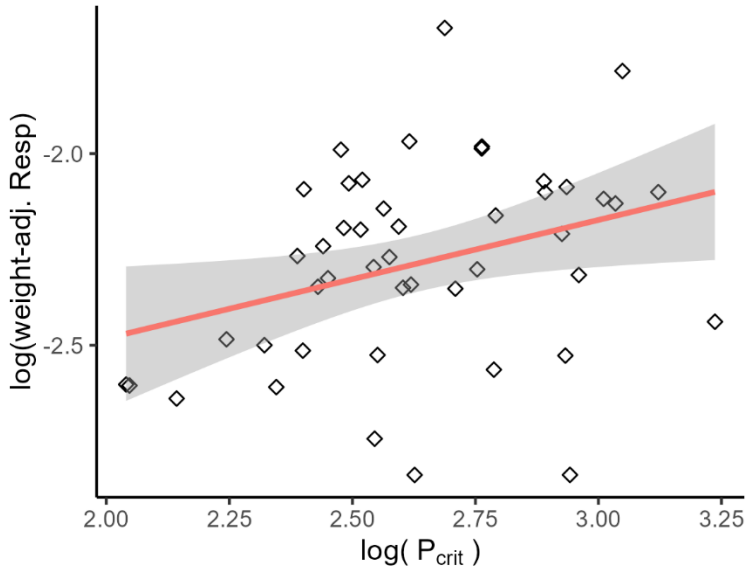

Figure S3. Linear regression between weight-adjusted respiration rates and P$_{crit}$ (model: log(P$_{crit}$) ~ log(weight_adj_rates).

Supplementary Tables

Table S1. Lead-210 dating of sediment core where *Daphnia* were hatched from.

Top of Interval (cm)	Base of Interval (cm)	Mid of Interval (cm)	Total 210Pb (pCi/g)	Error of Total Pb (±s.d.)	Cum. Dry Mass (g/cm2)	Unsup. 210Pb (pCi/g)	Error of Unsup Pb (±s.d.)	Age: Base of Int. (yr)	Error of Age (±s.d.)	Date: Base A.D.	Date: Mid A.D.	Sediment DMAR (g/cm2 yr)	Error of DMAR (±s.d.)
0	0.5	0.25	10.520	0.425	0.032	10.294	0.425	3.96	0.76	2018.4	2020.4	0.0081	0.0003
0.5	1	0.75	9.311	0.274	0.056	9.085	0.274	6.92	0.80	2015.4	2016.9	0.0082	0.0003
1	1.5	1.25	8.395	0.309	0.096	8.169	0.309	11.85	0.86	2010.5	2013.0	0.0081	0.0003
1.5	2	1.75	9.362	0.257	0.137	9.137	0.257	18.71	0.97	2003.6	2007.1	0.0060	0.0002
2	2.5	2.25	5.849	0.189	0.191	5.624	0.189	25.54	1.10	1996.8	2000.2	0.0079	0.0003
2.5	3	2.75	3.602	0.124	0.287	3.377	0.125	34.92	1.34	1987.4	1992.1	0.0102	0.0005
3	3.5	3.25	3.066	0.111	0.366	2.841	0.112	43.52	1.66	1978.8	1983.1	0.0092	0.0005
3.5	4	3.75	2.094	0.047	0.437	1.869	0.049	49.90	1.98	1972.4	1975.6	0.0111	0.0007
4	4.5	4.25	1.570	0.052	0.562	1.345	0.054	60.54	2.66	1961.8	1967.1	0.0118	0.0009
4.5	5	4.75	1.019	0.029	0.735	0.794	0.032	72.92	3.83	1949.4	1955.6	0.0140	0.0015
5	5.5	5.25	0.711	0.022	0.893	0.486	0.026	82.63	5.12	1939.7	1944.6	0.0162	0.0023
5.5	6	5.75	0.541	0.018	1.039	0.316	0.023	90.35	6.47	1932.0	1935.9	0.0190	0.0036
6	6.5	6.25	0.514	0.017	1.195	0.288	0.022	100.23	8.74	1922.1	1927.1	0.0158	0.0038
6.5	7	6.75	0.346	0.011	1.351	0.121	0.018	105.47	10.25	1916.9	1919.5	0.0297	0.0096
7	7.5	7.25	0.443	0.016	1.511	0.218	0.021	118.33	15.21	1904.0	1910.5	0.0125	0.0050
7.5	8	7.75	0.380	0.012	1.662	0.154	0.019	131.01	22.50	1891.3	1897.7	0.0119	0.0070
8	8.5	8.25	0.336	0.010	1.799	0.111	0.017	143.27	32.86	1879.1	1885.2	0.0112	0.0096

Table S2 Pair-wise dissimilarity matrix (1-IBS) between clones. Clone labels are coloured according to genetic cluster and subpopulation membership (see colour code in Figure S1).

	SS4-L20	SS4-L17	SS4-L10	SS4-L13	SS4-L22	SS4-L19	SS4-L11	SS4-L24	SS4-L28	SS4-32	SS4-31	SS4-30	SS4-5	SS4-L9	SS4-17	SS4-L3	SS4-L8	SS4-6A	SS4-26	SS4-15x	SS4-13X	SS4-21	SS4-23
SS4-L20	0	0.06922	0.06734	0.06567	0.06503	0.06257	0.06241	0.06068	0.06173	0.13333	0.13007	0.12857	0.12787	0.1279	0.12673	0.12343	0.12319	0.12162	0.12488	0.12346	0.12126	0.1092	0.11942
SS4-L17	0.06922	0	0.05577	0.05462	0.05374	0.05127	0.05055	0.04894	0.05017	0.12342	0.12053	0.11869	0.11801	0.11794	0.11699	0.11325	0.11279	0.11117	0.11521	0.11351	0.11101	0.09848	0.10937
SS4-L10	0.06734	0.05577	0	0.05206	0.05113	0.04877	0.04854	0.04669	0.0478	0.12136	0.11798	0.11655	0.11574	0.11576	0.11494	0.11101	0.11066	0.10901	0.11276	0.11114	0.10909	0.09633	0.10701
SS4-L13	0.06567	0.05462	0.05206	0	0.04993	0.04707	0.0468	0.04483	0.04601	0.12054	0.11709	0.11521	0.11447	0.11506	0.11346	0.10976	0.10932	0.10788	0.11201	0.10998	0.10782	0.09482	0.10566
SS4-L22	0.06503	0.05374	0.05113	0.04993	0	0.04622	0.0461	0.04411	0.04535	0.11982	0.11657	0.11475	0.11386	0.11404	0.11279	0.10905	0.10861	0.10697	0.1114	0.1093	0.10731	0.09432	0.10504
SS4-L19	0.06257	0.05127	0.04877	0.04707	0.04622	0	0.04331	0.04128	0.04247	0.1176	0.11433	0.11243	0.11178	0.11179	0.11084	0.10671	0.10645	0.10455	0.10927	0.10712	0.10467	0.0914	0.10268
SS4-L11	0.06241	0.05055	0.04854	0.0468	0.0461	0.04331	0	0.04055	0.04152	0.11741	0.1137	0.11177	0.11111	0.11092	0.10984	0.10646	0.10577	0.10403	0.10889	0.10711	0.10457	0.09125	0.10283
SS4-L24	0.06068	0.04894	0.04669	0.04483	0.04411	0.04128	0.04055	0	0.03987	0.11574	0.11195	0.10981	0.10936	0.10925	0.10807	0.10445	0.10396	0.10235	0.10723	0.10563	0.10306	0.08912	0.10113
SS4-L28	0.06173	0.05017	0.0478	0.04601	0.04535	0.04247	0.04152	0.03987	0	0.11675	0.113	0.111	0.11019	0.11023	0.10916	0.10569	0.10538	0.10355	0.10813	0.1063	0.10415	0.0902	0.10214
SS4-32	0.13333	0.12342	0.12136	0.12054	0.11982	0.1176	0.11741	0.11574	0.11675	0	0.07247	0.07044	0.06928	0.06963	0.06891	0.06432	0.06402	0.06242	0.11486	0.11241	0.11064	0.09915	0.10835
SS4-31	0.13007	0.12053	0.11798	0.11709	0.11657	0.11433	0.1137	0.11195	0.113	0.07247	0	0.06638	0.06544	0.06529	0.06433	0.06067	0.06009	0.05872	0.11105	0.10958	0.10741	0.09498	0.1056
SS4-30	0.12857	0.11869	0.11655	0.11521	0.11475	0.11243	0.11177	0.10981	0.111	0.07044	0.06638	0	0.06363	0.06384	0.06265	0.05887	0.05818	0.05691	0.1096	0.10792	0.10567	0.09304	0.10398
SS4-5	0.12787	0.11801	0.11574	0.11447	0.11386	0.11178	0.11111	0.10936	0.11019	0.06928	0.06544	0.06363	0	0.06304	0.06208	0.05812	0.05748	0.05595	0.10855	0.10689	0.10466	0.0923	0.10244
SS4-L9	0.1279	0.11794	0.11576	0.11506	0.11404	0.11179	0.11092	0.10925	0.11023	0.06963	0.06529	0.06384	0.06304	0	0.06183	0.05784	0.05747	0.05589	0.10901	0.10717	0.10492	0.09223	0.10315
SS4-17	0.12673	0.11699	0.11494	0.11346	0.11279	0.11084	0.10984	0.10807	0.10916	0.06891	0.06433	0.06265	0.06208	0.06183	0	0.05688	0.05646	0.05465	0.10796	0.10597	0.104	0.09149	0.10206
SS4-L3	0.12343	0.11325	0.11101	0.10976	0.10905	0.10671	0.10646	0.10445	0.10569	0.06432	0.06067	0.05887	0.05812	0.05784	0.05688	0	0.0522	0.05021	0.10441	0.10233	0.10037	0.08752	0.09811
SS4-L8	0.12319	0.11279	0.11066	0.10932	0.10861	0.10645	0.10577	0.10396	0.10538	0.06402	0.06009	0.05818	0.05748	0.05747	0.05646	0.0522	0	0.0495	0.10402	0.10196	0.09987	0.08698	0.09781
SS4-6A	0.12162	0.11117	0.10901	0.10788	0.10697	0.10455	0.10403	0.10235	0.10355	0.06242	0.05872	0.05691	0.05595	0.05589	0.05465	0.05021	0.0495	0	0.10208	0.10045	0.09823	0.08538	0.09626
SS4-26	0.12488	0.11521	0.11276	0.11201	0.1114	0.10927	0.10889	0.10723	0.10813	0.11486	0.11105	0.1096	0.10855	0.10901	0.10796	0.10441	0.10402	0.10208	0	0.07249	0.06994	0.05697	0.06804
SS4-15x	0.12346	0.11351	0.11114	0.10998	0.1093	0.10712	0.10711	0.10563	0.1063	0.11241	0.10958	0.10792	0.10689	0.10717	0.10597	0.10233	0.10196	0.10045	0.07249	0	0.06813	0.05514	0.06521
SS4-13X	0.12126	0.11101	0.10909	0.10782	0.10731	0.10467	0.10457	0.10306	0.10415	0.11064	0.10741	0.10567	0.10466	0.10492	0.104	0.10037	0.09987	0.09823	0.06994	0.06813	0	0.0523	0.06319
SS4-21	0.1092	0.09848	0.09633	0.09482	0.09432	0.0914	0.09125	0.08912	0.0902	0.09915	0.09498	0.09304	0.0923	0.09223	0.09149	0.08752	0.08698	0.08538	0.05697	0.05514	0.0523	0	0.05002
SS4-23	0.11942	0.10937	0.10701	0.10566	0.10504	0.10268	0.10283	0.10113	0.10214	0.10835	0.1056	0.10398	0.10244	0.10315	0.10206	0.09811	0.09781	0.09626	0.06804	0.06521	0.06319	0.05002	0

Table S3. Post-hoc test among genetic clusters for gen1(T_{imm} ~ Genetic Cluster + (1|Run)) for T_{imm} data using Holm method.

Gen. cluster comparison	Estimate	Std. Error	z value	Pr(>|z|)
mixed - historical	-158.3	250.5	-0.63	0.527
modern -historical	-1271.1	255.7	-4.97	**1.33E-06**
modern - mixed	-1112.8	62.8	-6.84	**2.45E-11**

Table S4. Post-hoc test among genetic clusters (for ANOVA model Pcrit ~ genetic cluster) for P_{crit} using Holm method.

Gen. cluster comparison	Estimate	Std. Error	t value	Pr(>|t|)
mixed - historical	1.72	1.86	0.93	0.621
modern -historical	4.65	1.87	2.49	**0.042**
modern - mixed	2.93	1.17	2.51	**0.040**